

Geophysical Research Letters

RESEARCH LETTER

10.1029/2020GL091747

Key Points:

- Dissipation in the central Arctic has nearly doubled in summer while declining in winter; no interannual trends are found in any region
- Summer heat flux in the central Arctic has risen by an order of magnitude due to stronger and more prevalent internal wave-driven mixing
- The eastern Arctic appears particularly vulnerable to accelerated sea-ice melt due to the strengthening “ice/internal-wave” feedback

Supporting Information:

Supporting Information may be found in the online version of this article.

Correspondence to:

H. V. Dosser,
hdosser@eoas.ubc.ca

Citation:

Dosser, H. V., Chanona, M., Waterman, S., Shibley, N. C., & Timmermans, M.-L. (2021). Changes in internal wave-driven mixing across the Arctic Ocean: Finescale estimates from an 18-year pan-Arctic record. *Geophysical Research Letters*, *48*, e2020GL091747. <https://doi.org/10.1029/2020GL091747>

Received 16 NOV 2020
Accepted 29 MAR 2021

Changes in Internal Wave-Driven Mixing Across the Arctic Ocean: Finescale Estimates From an 18-Year Pan-Arctic Record

H. V. Dosser¹ , M. Chanona¹ , S. Waterman¹ , N. C. Shibley² , and M.-L. Timmermans² 

¹Department of Earth, Ocean and Atmospheric Sciences, University of British Columbia, Vancouver, British Columbia, Canada, ²Department of Earth and Planetary Sciences, Yale University, New Haven, CT, USA

Abstract The Arctic climate is changing rapidly, with dramatic sea ice declines and increasing upper-ocean heat content. While oceanic heat has historically been isolated from the sea ice by weak vertical mixing, it has been hypothesized that a reduced ice pack will increase energy transfer from the wind into the internal wave (IW) field, enhancing mixing and accelerating ice melt. We evaluate this positive ice/internal-wave feedback using a finescale parameterization to estimate dissipation, a proxy for the energy available for IW-driven mixing, from pan-Arctic hydrographic profiles over 18 years. We find that dissipation has nearly doubled in summer in some regions. Associated heat fluxes have risen by an order of magnitude, underpinned by increases in the strength and prevalence of IW-driven mixing. While the impact of the ice/internal-wave feedback will likely remain negligible in the western Arctic, sea-ice melt in the eastern Arctic appears vulnerable to the feedback strengthening.

Plain Language Summary The Arctic is changing rapidly, with dramatic declines in sea ice and warming of upper-ocean waters. Historically, weak ocean mixing has prevented the melting of sea ice by oceanic heat. Scientists have hypothesized that as sea ice melts and open water is exposed to the wind, more energetic internal waves will result. These waves cause mixing in the upper ocean, which can bring heat upwards to the surface and melt more sea ice, thus creating a positive feedback loop. To test the importance of this feedback, we use ocean measurements to estimate “dissipation,” a proxy for the internal wave energy that is available to cause mixing. The measurements cover much of the Arctic Ocean for the years 2002–2019. We find that dissipation has increased during summer in recent years. Summer heat transport toward the sea ice has also increased, on average by a factor of 10, as internal wave-driven mixing became stronger and more prevalent. We estimate that the western Arctic is unlikely to experience significant future sea-ice melt due to this positive feedback; however, the eastern Arctic may be vulnerable to accelerated sea-ice melt as increases in dissipation continue.

1. Introduction

The strength of mixing in the Arctic Ocean is an important control on the ability of heat in the ocean interior to penetrate the stratified upper ocean below the sea ice (D’Asaro & Morison, 1992). However, our understanding of mixing in the Arctic Ocean is arguably the most limited of all regions of the world ocean. As a consequence, the spatiotemporal variability of heat loss from inflowing Atlantic and Pacific waters is not well known (e.g., Lenn et al., 2009; Lincoln et al., 2016). In particular, observations of mixing in the Arctic Ocean are scarce, with direct (i.e., microstructure) inferences of ocean mixing being limited both temporally and geographically. In large-scale studies of ocean mixing rates inferred using indirect methods (Kunze, 2017; Kunze et al., 2006; Waterhouse et al., 2014; Whalen et al., 2012, 2018, 2020), data from the Arctic Ocean are notably absent. There is thus a need to more robustly quantify Arctic Ocean mixing metrics in order to improve our understanding of the role of upper-ocean mixing in vertical heat transport and sea-ice decline.

In the central Arctic Ocean basins, the limited measurements available consistently show an environment characterized by low mixing rates, associated with low internal wave (IW) energy levels and low turbulent kinetic energy dissipation rates (hereafter “dissipation”) (D’Asaro & Morison, 1992; Fer, 2009; Guthrie et al., 2013; Rainville & Winsor, 2008). This weak mixing has been attributed to a combination of extensive year-round sea-ice cover, strong upper-ocean stratification (Rainville et al., 2011), and weak tidal flow

(Kowalik & Proshutinsky, 2013). As a consequence, upward mixing of heat stored in near-surface Atlantic-sourced or Pacific-sourced waters has been suppressed (Rudels et al., 1996; Toole et al., 2010). However, over the past few decades, sea-ice thickness and extent have decreased significantly (Kwok, 2018; Perovich & Richter-Menge, 2009; Stroeve et al., 2012) and sea-ice drift speeds have increased (Kwok et al., 2013). It has been speculated that such changes in Arctic sea-ice conditions could result in enhanced transfer of wind energy across the air-ocean interface, forcing more energetic wind-generated internal waves (Dosser & Rainville, 2016; Martini et al., 2014; Rainville & Woodgate, 2009). These waves are ultimately expected to break in the stratified water column, with the potential to intensify vertical mixing and enhance upward heat transport, thus resulting in further sea-ice melt (Carmack et al., 2015). This positive ice/internal-wave feedback may additionally be strengthened by increases in Arctic Ocean heat content. Observations have indicated a doubling of ocean heat content in the Pacific Water between 1987 and 2017 (Timmermans et al., 2018), as well as a warming and shoaling of the Atlantic Water in recent decades (Polyakov et al., 2017). While recent studies suggest that strong stratification continues to limit IW-driven mixing and associated heat fluxes in the western Arctic (Guthrie et al., 2013; Lincoln et al., 2016), other work points to locally enhanced mixing and heat fluxes in the eastern Arctic where the upper-ocean stratification has weakened (Polyakov, Rippeth, Fer, Alkire, et al., 2020; Polyakov, Rippeth, Fer, Baumann, et al., 2020).

Given the scarcity of direct measurements of ocean mixing, the finescale parameterization of turbulent dissipation provides an important tool to quantify mixing over a broad range of space and time scales. This method provides an opportunity to investigate mixing variability using readily available data sets such as that collected by the global Argo float network (Whalen et al., 2012, 2018, 2020). Estimates of dissipation derived from the finescale parameterization have been shown to agree well with direct measurements; Whalen et al. (2015) find agreement within a factor of 2–3 for 96% of comparisons using Argo data obtained from diverse regions of varying topography and oceanic flow conditions. In the Arctic Ocean, comparisons with direct measurements show similar levels of agreement (Fer et al., 2010; Fine et al., 2021; Guthrie et al., 2013; Kawaguchi et al., 2016), providing confidence that the parameterization can be successfully applied in a range of Arctic conditions.

In this study, we analyze Ice-Tethered Profiler (ITP) data (Krishfield et al., 2008; Toole et al., 2011) and hydrographic profiles from the Arctic continental shelf and slope to provide the most complete characterization of the Arctic Ocean mixing environment to date. Using this 18-year pan-Arctic observational record, we examine mixing variability on previously inaccessible time scales, assessing seasonal to interannual variability with unprecedented statistical rigor and spatial coverage. We quantify changes in IW-driven dissipation and associated diffusivity, heat flux, and sea-ice melt in order to assess the importance of the hypothesized ice/internal-wave feedback. Lastly, we investigate the vulnerability of sea ice to plausible future changes in IW-driven dissipation.

2. Data and Methods

2.1. Observational Data

We analyze 29,074 hydrographic profiles from 89 ITPs that sampled the central Arctic Ocean year-round between 2004 and 2019 and 3,084 hydrographic profiles collected by multiple ship-based programs in Canadian Arctic shelf and slope waters between 2002 and 2014; the latter provide a useful comparison between the continental shelf and the central basins sampled by the ITPs. We focus our analysis on the Canada Basin (CB), the Eurasian Basin (EB), and the Canadian Arctic shelf (Shelf) (Figure 1 upper inset and supporting information). ITP profiles are collected at least twice per day between ~7-m and ~750-m depth and take <1 h to complete, allowing us to treat individual profiles as snapshots of the internal wavefield at a fixed location. Data used are an extension of those described in Dosser and Rainville (2016), processed from raw ITP temperature and conductivity data sampled at 1 Hz and binned to 1 db. Processing follows the steps developed by Krishfield et al. (2008) and data are comparable to the fully processed product (provided at www.whoi.edu/itp), which included instruments up to ITP61 at the time of our analysis. Although ITPs are connected to a surface buoy moored in a perennial ice floe, they frequently sample mobile ice packs with concentrations below 20% in summer (Dosser & Rainville, 2016). The Shelf data, sampled at 24 Hz and binned to 1 db, were collected year-round, with 2–3 times more profiles available per month for late summer/early fall (Jul-Oct) compared to other months (see Chanona et al. (2018) for technical details). Note

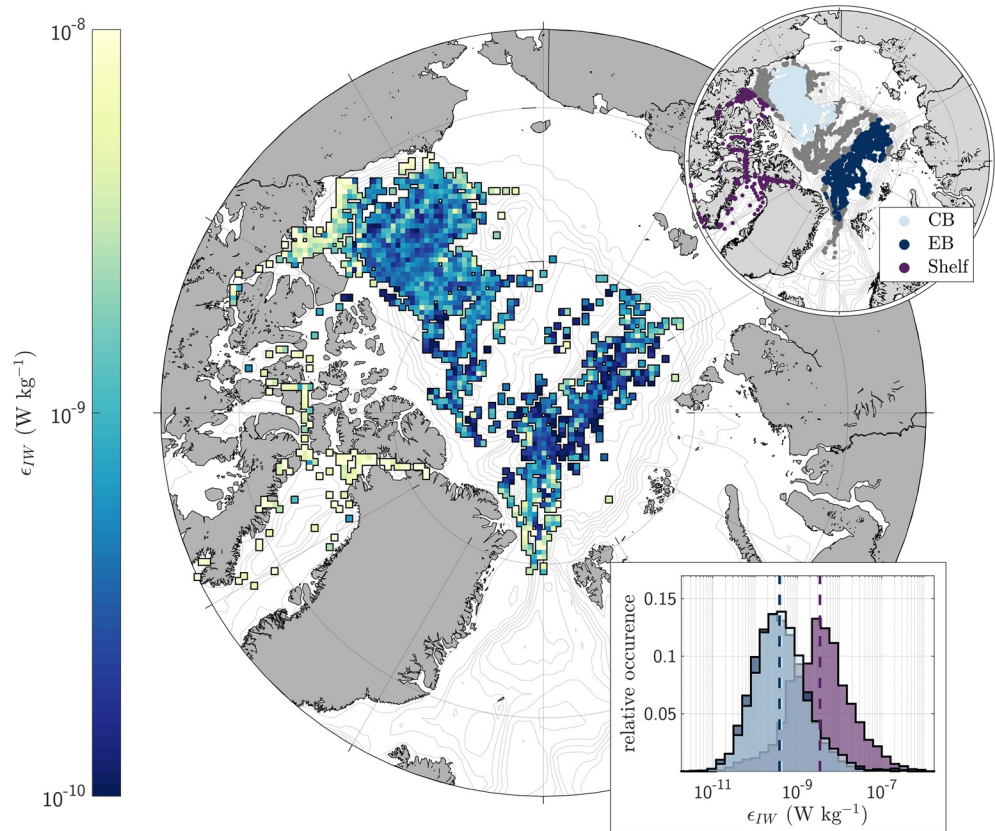


Figure 1. Spatial map and regional distributions of IW-driven dissipation. Estimates of ϵ_{IW} from the 128-m segment of the water column below the mixed layer, and excluding profile segments containing double-diffusive staircase features, are shown. In the map, values spanning the 18-year record (2002–2019) are geometrically averaged into grid cells with a mean size of 36×36 km. The upper inset delineates profile locations within each of the three regions discussed in the text: Canada Basin (CB), Eurasian Basin (EB), and Canadian Arctic shelf (Shelf). The lower inset shows the distribution of individual ϵ_{IW} estimates in each of these regions along with the corresponding geometric mean values (dashed lines). IW, internal wave.

that for 2002–2004, Shelf data collection was heavily biased to the southeastern Beaufort Sea/Amundsen Gulf, and lacked measurements from the most energetic regions of the Canadian Arctic Archipelago.

2.2. Finescale Parameterization for Dissipation

We estimate the IW-driven turbulent kinetic energy dissipation rate, ϵ_{IW} , by applying a strain-based finescale parameterization, which is based on theory describing the downscale spectral energy cascade between internal wave scales and the turbulent microscales where dissipation and mixing occur (see Polzin et al. (2014) for a review). The implementation applied here is identical to that in Chanona et al. (2018), which closely follows that of Whalen et al. (2012) and builds off earlier formulations (Gregg, 1989; Polzin et al., 1995). Strain is computed relative to the background stratification in the stratified water column below the mixed layer. We approximate the background stratification for each stratification profile by first removing the mixed layer and then using a smooth piecewise quadratic fit. We compute strain from the stratification profile, N^2 , as $(N^2 - N_{ref}^2)/N_{ref}^2$, where N_{ref}^2 represents the depth-varying fit to the background stratification. To calculate strain variance, we apply a discrete Fourier transform to 75% overlapping 128-m segments of each profile, again excluding the mixed layer. Resulting spectra are integrated between vertical wavenumbers of 0.02 and 0.10 cpm, corresponding to vertical wavelengths of 10–50 m. The spectra are white on average over this integration range (supporting information), as expected in an equilibrated internal wavefield suitable for application of the parameterization (Polzin et al., 2014). We assume a constant shear-to-strain

ratio, R_ω , of 7 (the global average in Kunze et al. (2006)). There is some evidence that the Arctic Ocean is characterized by values of R_ω larger than this global average value (Fine et al., 2021; Guthrie et al., 2013). However, an analysis of uncertainty accounting for a potential systematic underestimation in ϵ_{IW} resulting from our choice of R_ω indicates that this underestimation is limited to a factor of 2 on average (supporting information). The estimates of ϵ_{IW} that we obtain correspond to 128-m segments of each profile and have a 32-m depth resolution. Here, we consider only the shallowest ϵ_{IW} estimate in each profile (i.e., those that are most relevant to sea-ice melt by upper-ocean heat); this comprises 16,466 estimates centered at 64 m below the base of the mixed layer.

When applying the finescale parameterization in the Arctic Ocean, it is critical to first identify and exclude profile segments containing double-diffusive staircase-like features, as application of the method is not appropriate when mixing is driven by processes other than breaking of the local internal wavefield (such as double diffusion). Double-diffusive staircases are caused by a small-scale diffusive-convective mixing process and are prevalent throughout the Arctic basins (Shibley et al., 2017; Sirevaag & Fer, 2012; Timmermans et al., 2008). We identify 128-m profile segments that contain staircase-like features by following the methodology in Shibley et al. (2017). Here, we adjust the parameters used such that both well-defined and marginally staircase-like features are identified. Specifically, we examine a larger vertical depth interval (50 m) above the Atlantic Water temperature maximum and require staircase-like features to be present over a smaller fraction of the depth examined (at least 4 m). We visually confirm that our criteria successfully identify these features in all regions considered. In the 128-m profile segment below the mixed layer considered here, staircase-like features are absent in 58% of profiles, making these segments suitable for application of the finescale parameterization.

3. Spatiotemporal Variability of Dissipation

When viewed as a spatial map, our ϵ_{IW} estimates provide the most well-resolved pan-Arctic view of IW-driven dissipation in the upper ocean to date (Figure 1). The comprehensive spatial coverage highlights large-scale patterns of enhanced dissipation near continental boundaries and sloping topography and lower values over smooth basin topography, consistent with previous studies (D'Asaro & Morison, 1992; Rainville & Winsor, 2008; Rippeth et al., 2015). Dissipation in the central Arctic basins is typically an order of magnitude less than that on the continental shelf, with regional geometric mean values (characterizing the central tendency of a log-normally distributed quantity) of $(4.2 \pm 0.1) \times 10^{-10} \text{ W kg}^{-1}$ in the CB and $(3.8 \pm 0.1) \times 10^{-10} \text{ W kg}^{-1}$ in the EB vs. $(3.4 \pm 0.1) \times 10^{-9} \text{ W kg}^{-1}$ on the Shelf (Figure 1, lower inset). (Error bounds provide a measure of the uncertainty in reported average values resulting from random uncertainty in ϵ_{IW} estimates; see supporting information for details). Our regional distributions of ϵ_{IW} are consistent with the range of values reported in previous localized studies in the Arctic Ocean from both direct (i.e., microstructure) and indirect (i.e., parameterized) methods (Chanona et al., 2018; Fer, 2009; Fer et al., 2010; Fine et al., 2021; Kawaguchi et al., 2016; Lenn et al., 2009; Lincoln et al., 2016; Rippeth et al., 2015). As at lower latitudes (Whalen et al., 2018), there is multiple-order-of-magnitude variability in the full ϵ_{IW} distribution, with a 1–99% interpercentile range of 2×10^{-11} to $1 \times 10^{-7} \text{ W kg}^{-1}$. Our estimates appear to robustly capture well-sampled distributions of Arctic Ocean IW-driven dissipation, an inherently patchy and intermittent process. The large number of estimates available, combined with their temporal resolution, thus permits a meaningful regional examination of temporal variability on previously inaccessible time scales.

When viewed as a time series, profiles spanning 16 years in the CB (2004–2019), 10 years in the EB (2007–2016), and 13 years on the Shelf (2002–2014) allow us to quantify seasonal to interannual variability and long-term trends. Despite expectations that climatic changes witnessed in the Arctic Ocean in recent decades could lead to steady increases in IW-driven dissipation, time series of monthly averaged ϵ_{IW} show no evidence of a statistically significant linear trend in the CB, EB, or on the Shelf over the years spanned by the record (Figure 2). However, this view does suggest that the seasonal cycle in each of the basins has become more pronounced in the latter part of the record (2011 onwards, hereafter “later period”). We investigate this shift in detail in the CB, where the spatial and temporal coverage of the observational record is most extensive. Here, estimates of ϵ_{IW} peak during late summer (July and August, hereafter “summer”) as the sea ice approaches its minimum annual extent, then decrease to a minimum in late winter (March and April, hereafter “winter”) when the sea-ice extent is maximal and the ice pack is least mobile (Figure 3). We note



Figure 2. Time series of monthly averaged dissipation showing no statistically significant linear interannual trends. Markers show geometric monthly averaged values of ϵ_{IW} in the (a) CB, (b) EB, and (c) Shelf. Marker size indicates the number of estimates, n , used in each average (averages that include less than five estimates are excluded). Solid and dashed lines show a linear fit and its 95% confidence interval respectively, with values for the slope and its 95% confidence interval provided in the upper left corner in units of orders of magnitude increase per year. CB, Canada Basin; EB, Eurasian Basin; Shelf, Canadian Arctic shelf.

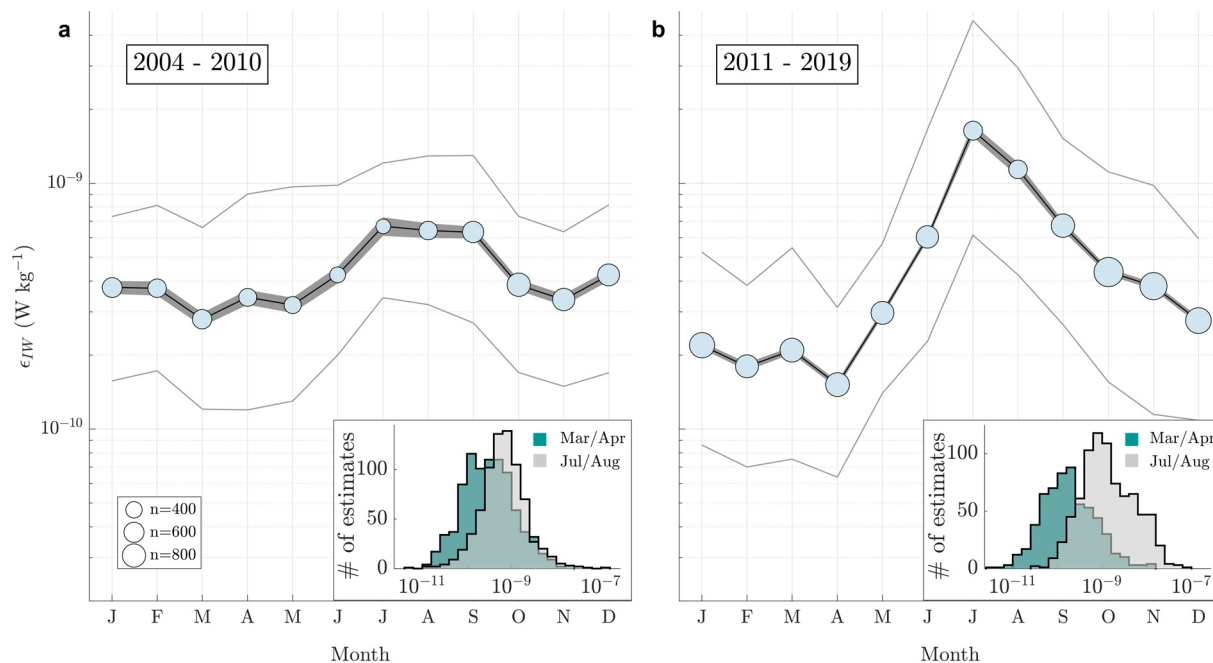


Figure 3. Seasonal cycle in dissipation in the CB. Geometric monthly averages of ϵ_{IW} in the CB for the periods (a) 2004–2010 and (b) 2011–2019. Marker size indicates the number of estimates, n , used in each average and the gray lines provide the interquartile range. Gray shading indicates the error bounds for random uncertainty (see supporting information). Insets provide the associated distributions of individual ϵ_{IW} estimates for the months of March and April (winter) in teal and July and August (summer) in gray. CB, Canada Basin.

that the seasonal timing of elevated ϵ_{IW} in summer is likely related to sea-ice properties in the immediate vicinity of the ITPs and as such, this timing may differ in other regions or for the Canada Basin as a whole.

We find that the magnitude of this seasonal cycle is enhanced in the later period, caused primarily by an increase in summer; the geometric mean of the summer ϵ_{IW} distribution from 2011 to 2019 has doubled relative to that of the 2004–2010 distribution. We note that despite this increase, and consistent with the lack of interannual trend, the 1–99% interpercentile range of all (year-round) ϵ_{IW} estimates does not change significantly between the earlier and later period, spanning $\mathcal{O}(10^{-11})$ W kg⁻¹ to $\mathcal{O}(10^{-8})$ W kg⁻¹ in both cases. Rather, values in summer tend to become higher, while values in winter tend to become lower (Figure 3, insets). A similar examination of the ϵ_{IW} distributions in the less well-sampled EB reveals a smaller summer increase by a factor of 1.4 between the 2007–2010 and 2011–2016 periods (supporting information). Our uncertainty analysis suggests the relative increases in summer ϵ_{IW} values reported for both the CB and EB are robust (supporting information).

We suggest that an increased transfer of wind energy through a sparser, more mobile ice pack in recent years may be driving the reported summer ϵ_{IW} increase in the later period, while the corresponding winter reduction in ϵ_{IW} may be caused by reduced wind-ice-ocean drag in response to the loss of thick, multiyear ice floes (Cole et al., 2017; Martin et al., 2016). The increase in summer ϵ_{IW} values is consistent with the operation of the hypothesized ice/internal-wave feedback in the central basins, potentially in response to changes in summer sea-ice properties. Additionally, our ϵ_{IW} estimates for later summers may be biased low, given that ITPs are less likely to sample fully ice-free waters and that open water in the central basins has significantly increased in recent years. Thus, as Arctic sea-ice loss continues, ongoing increases in summer ϵ_{IW} appear likely.

4. Disproportionate Response of Diffusivity and Heat Flux to Changes in Dissipation

Given this evidence of increased IW-driven dissipation in the central basins during summer in recent years, it is critical to determine if an associated meaningful increase in the IW-driven diffusivity, κ_{IW} , and vertical heat flux, F_h , has occurred. In the low-energy, strongly stratified Arctic Ocean mixing environment, internal wave energy levels are expected to often be insufficient to overcome the background stratification and generate overturning; thus not all estimates of ϵ_{IW} are expected to contribute to IW-driven mixing. Further, we expect the efficiency of IW-driven mixing to be modified in conditions where the turbulence is strongly influenced by the stratification (Bouffard & Boegman, 2013; Ivey et al., 2008). To determine how to appropriately specify the diffusivity, we combine our estimates of ϵ_{IW} with the 128-m segment-averaged stratification, N^2 , to calculate the nondimensional buoyancy Reynolds number: $Re_B = \epsilon_{IW} / (\nu N^2)$, where ν is the kinematic viscosity of seawater (Figure 4a for the CB). We use Re_B , which is a measure of the destabilizing effects of turbulence relative to the stabilizing effects of stratification, to delineate three different mixing regimes (see also supporting information):

1. a “fully turbulent” IW-driven mixing regime ($Re_B \geq 20$) for which we specify the diffusivity according to the Osborn relation (Osborn, 1980)
2. a “marginal” IW-driven mixing regime ($1 < Re_B < 20$) for which we use a modified Osborn relation to account for a decrease in mixing efficiency (Bouffard & Boegman, 2013); and
3. a molecular mixing regime ($Re_B \leq 1$) for which we assume that energy associated with internal wave breaking is incapable of perturbing the stratification and thus mixing occurs at the rate of molecular diffusion (i.e., $\kappa_T = 1 \times 10^{-7}$ m² s⁻¹ for heat).

We denote the percentage of estimates in the two IW-driven mixing regimes by α_{IW} , which describes the prevalence of IW-driven mixing relative to all estimates including those in the molecular regime. As κ_{IW} is often orders of magnitude larger than κ_T , changes in either κ_{IW} or α_{IW} can have a disproportionate impact on the average heat flux. This treatment of IW-driven mixing, which includes consideration of both its strength and prevalence, is particularly important in the predominantly quiescent Arctic Ocean, where many ϵ_{IW} estimates correspond to marginal or molecular mixing regimes.

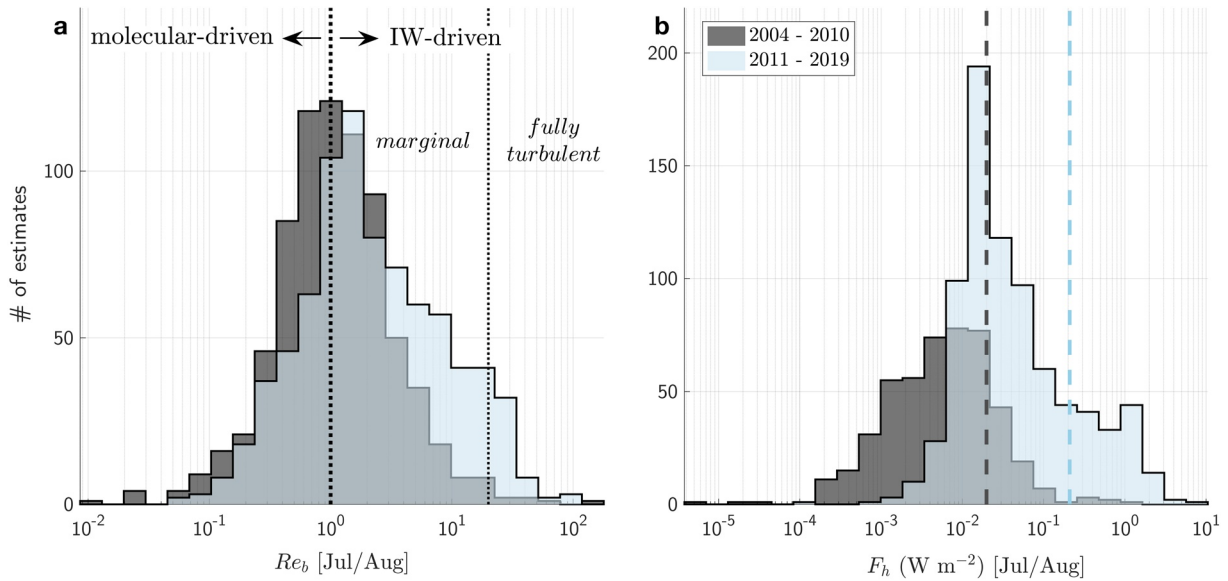


Figure 4. Shift in mixing regimes and vertical heat fluxes in the CB in summer. Distributions of (a) the buoyancy Reynolds number, Re_b , and (b) the vertical heat flux, F_h , associated with both molecular-driven and IW-driven mixing in the CB during the months of July and August for the periods 2004–2010 (gray) and 2011–2019 (pale blue). Dotted lines in (a) indicate $Re_b = 1$ (denoting the separation between the molecular-driven and IW-driven mixing regimes) and $Re_b = 20$ (denoting the separation between the marginal and fully turbulent IW-driven mixing regimes). Dashed lines in (b) give the average values of each distribution, $\overline{F_h}$. CB, Canada Basin; IW, internal wave.

Focusing on the summer in the central Arctic, we compute changes in the IW-driven diffusivity, κ_{IW} , the prevalence of IW-driven mixing, α_{IW} , and the average vertical heat flux, $\overline{F_h}$, between the earlier and later period (supporting information). In the CB, the geometric mean value of κ_{IW} increases from $(3 \pm 1) \times 10^{-7}$ to $(7 \pm 1) \times 10^{-7} \text{ m}^2 \text{ s}^{-1}$ and α_{IW} rises from $53 \pm 2\%$ to $73 \pm 2\%$ (with the subset of estimates representing fully turbulent mixing, i.e., $Re_b \geq 20$, rising from $1 \pm 1\%$ to $7 \pm 1\%$). In the EB, κ_{IW} increases from $(7 \pm 2) \times 10^{-7}$ to $(12 \pm 3) \times 10^{-7} \text{ m}^2 \text{ s}^{-1}$, α_{IW} remains roughly constant ($83 \pm 3\%$ to $80 \pm 3\%$), and fully turbulent estimates rise from $2 \pm 2\%$ to $8 \pm 2\%$. Since N^2 in summer does not exhibit meaningful changes over the record in either region (supporting information), these changes in κ_{IW} and α_{IW} are predominantly a result of changes in ϵ_{IW} . These increases in the strength and prevalence of IW-driven mixing drive disproportionate increases in $\overline{F_h}$; whereas corresponding average values of ϵ_{IW} increase by a factor of 2.1 in the CB and by a factor of 1.4 in the EB, $\overline{F_h}$ increases by an order of magnitude in both basins, rising from 0.020 ± 0.004 to $0.21 \pm 0.04 \text{ W m}^{-2}$ in the CB (Figure 4b) and from 0.2 ± 0.1 to $2 \pm 1 \text{ W m}^{-2}$ in the EB (not shown). In the CB, this increase in $\overline{F_h}$ is also the result of larger temperature gradients during the later period, with the average gradient increasing by a factor of 3 between the two periods (supporting information). In the EB, as the average temperature gradient remains approximately constant over the record, the order of magnitude increase in $\overline{F_h}$ is caused solely by the increase in ϵ_{IW} . We note, however, that the distributions of summer ϵ_{IW} estimates in the EB are less well-resolved (supporting information). Our uncertainty analysis indicates that the potential systematic underestimation of ϵ_{IW} may result in significant underestimation of κ_{IW} , α_{IW} , and F_h . Our reported values should thus be viewed as conservative estimates. Despite this, conclusions about relative changes in these metrics between the earlier and later periods are found to be robust (supporting information).

5. Future Increases in Dissipation and the Ice/Internal-Wave Feedback

While these *relative* increases in the average heat flux are substantial, they remain small in the context of the upper-ocean heat budget for the central Arctic. Specifically, despite the order of magnitude increase in $\overline{F_h}$ associated with increasing dissipation in recent years, the average values remain at least an order of magnitude smaller than the $\mathcal{O}(10) \text{ W m}^{-2}$ heat flux associated with solar heating of surface waters, which drives the majority of subsurface summer sea-ice melt (Timmermans, 2015; Timmermans et al., 2011). While a small number of the individual IW-driven heat flux estimates are $\mathcal{O}(10) \text{ W m}^{-2}$, calculating sea-ice melt

rates using the full distribution of these heat flux estimates from the later period demonstrates a potential to melt only 0.3 ± 0.1 cm of sea ice in the CB and 3 ± 2 cm in the EB over any 2-month summer period (supporting information). These results indicate that the increased strength and prevalence of IW-driven mixing in the central basins seen in recent years are still too low to bring sufficient oceanic heat to the surface to melt meaningful quantities of sea ice, even when uncertainties in ϵ_{IW} are considered. We conclude that the ice/internal-wave feedback has had a limited influence to date in the central Arctic basins.

The observed increase in summer IW-driven heat fluxes motivates us, however, to ask the question: *What future increase in dissipation is required for heat fluxes from stored oceanic heat to play a meaningful role in the ice/internal-wave feedback in the central Arctic basins?* To gain insight, we compute the shift in the observed distribution of summer ϵ_{IW} estimates from the later period that would be required to increase the associated $\overline{F_h}$ to 10 W m^{-2} , i.e., to a similar magnitude as the solar heating term in the upper-ocean heat budget. For this simple calculation, we assume no change in the corresponding distributions of vertical temperature gradient, density, or stratification, but recognize that future climate changes as well as changes in the mixing environment itself may cause changes in these fields. We find that to meaningfully contribute to the upper-ocean heat budget, estimates of ϵ_{IW} would need to increase by a factor of 40 in the CB, but by only a factor of 6 in the EB. Under this scenario, both basins would experience frequent and widespread IW-driven mixing ($\alpha_{IW} = 100\%$ in the CB and 99% in the EB, with fully turbulent mixing occurring 87% and 51% of the time, respectively). Associated heat fluxes would be capable of melting up to 17 cm of ice over a 2-month period, a significant fraction of the average thickness of September Arctic sea ice in recent years (typically 0.5–1.5 m (Kwok, 2018)).

The average value of ϵ_{IW} required in this scenario is an order of magnitude higher in the CB than in the EB, a disparity that reflects the contrast in upper-ocean stratification between basins, which is on average 3 times stronger in the CB (supporting information). These differing sensitivities are consistent with recent studies that suggest strong upper-ocean stratification continues to limit IW-driven overturns in the CB (Guthrie et al., 2013; Lincoln et al., 2016), while heat flux and IW shear appear to be increasing in summer in the eastern EB where stratification has locally weakened (Polyakov, Rippeth, Fer, Alkire, et al., 2020; Polyakov, Rippeth, Fer, Baumann, et al., 2020). Our results suggest that IW-driven mixing in the CB is unlikely to contribute significantly to sea-ice melt for the foreseeable future, provided the current upper-ocean stratification is maintained. In the EB, by contrast, we estimate that an $\mathcal{O}(10) \text{ W m}^{-2}$ average heat flux can be realized with a much smaller increase in ϵ_{IW} . Should the trends of weakening stratification and increasing IW-driven shear reported on the slope in the eastern EB by Polyakov, Rippeth, Fer, Baumann, et al. (2020) be realized basin-wide, it is plausible that the EB could transition from a quiescent environment with mixing hotspots over sloping topography (e.g., Rippeth et al., 2015) to a more energetic state with accelerated declines in summer sea-ice.

6. Summary

We use an 18-year pan-Arctic observational record and a finescale parameterization to assess the importance of the ice/internal-wave feedback. We find that several processes associated with this positive feedback have increased across the central Arctic basins in recent summers, and note that increases in IW-driven mixing have caused disproportionate increases in heat flux. Though the increased heat fluxes have had the potential for only a modest impact on sea-ice melt to date, we estimate that regions with sufficiently low stratification, such as the eastern Arctic, are vulnerable to accelerated sea-ice melt as the feedback strengthens. It is therefore critical to track future changes in IW-driven mixing, as well as changes in stratification and temperature gradient that directly influence diffusivity and heat flux. As IW-driven mixing is an inherently inhomogeneous and sporadic process, this will necessitate ongoing observational records, such as those from Ice-Tethered Profilers, that sample over long durations and large geographic areas. Robustly quantifying both the strength and prevalence of IW-driven mixing is of particular importance since we have identified these metrics as key factors in setting the total upward heat flux from stored oceanic heat. As the melt season lengthens, freeze-up is delayed, multiyear ice disappears, and previous records for minimum ice extent are broken monthly (Andersen et al., 2020), tracking increases in IW-driven mixing is necessary to effectively predict and respond to future changes in the Arctic Ocean environment.

Data Availability Statement

The Ice-Tethered Profiler data were collected and made available by the Ice-Tethered Profiler program (Kris-hfield et al., 2008; Toole et al., 2011) based at the Woods Hole Oceanographic Institution (WHOI; www.whoi.edu/itp). They can be accessed at <ftp://ftp.whoi.edu/whoinet/itpdata>. The Canadian Arctic shelf data were collected on Canadian research icebreakers the *CCGS Amundsen*, the *CCGS Pierre Radisson*, the *CCGS Sir Wilfrid Laurier*, and the *CCGS Louis St. Laurent*. They were made available by the ArcticNet science program, which is supported by the Canada Foundation for Innovation and the Natural Sciences and Engineering Research Council of Canada (NSERC), and by the Beaufort Gyre Exploration Program based at WHOI. They can be accessed at www.polardata.ca.

Acknowledgments

This work was funded by the Natural Sciences and Engineering Research Council of Canada (NSERC) through the Canadian Arctic GEOTRACES Program supported by the Climate Change and Atmospheric Research Program (NSERC RGPC 433848-12) and the Discovery Grants Program (NSERC-2015-04866 and NSERC-2020-05799), and by the National Science Foundation (NSF) Office of Polar Programs (Award 1950077). M. Chanona was further supported by the Earth, Ocean and Atmospheric Sciences Department at the University of British Columbia (UBC); the Vanier Canada Graduate Scholarships program; the Killam Doctoral Scholarships program; and the UBC Four Year Fellowship Program. N. C. Shibley was supported by the U.S. Department of Defense through the National Defense Science and Engineering Graduate Fellowship Program. We appreciate support associated with the NSF Forum for Arctic Modeling and Observational Synthesis (FAMOS), where this project was first conceived. We wish to thank Dr. Effie Fine for helpful discussions that contributed greatly to the rigor of our uncertainty analysis. Additionally, we thank two anonymous reviewers for their constructive comments, which resulted in an improved manuscript.

References

Andersen, J. K., Andreassen, L. M., Baker, E. H., Ballinger, T. J., Berner, L. T., Bernhard, G. H., et al. (2020). The Arctic [in “State of the Climate in 2019”]. *Bulletin of the American Meteorological Society*, 101(8), S239–S286. <https://doi.org/10.1175/BAMS-D-20-0086.1>

Bouffard, D., & Boegman, L. (2013). A diapycnal diffusivity model for stratified environmental flows. *Dynamics of Atmospheres and Oceans*, 61–62, 14–34. <https://doi.org/10.1016/j.dynatmoce.2013.02.002>

Carmack, E., Polyakov, I., Padman, L., Fer, I., Hunke, E., Hutchings, J., et al. (2015). Toward quantifying the increasing role of oceanic heat in sea ice loss in the New Arctic. *Bulletin of the American Meteorological Society*, 96(12), 2079–2105. <https://doi.org/10.1175/BAMS-D-13-00177.1>

Chanona, M., Waterman, S., & Gratton, Y. (2018). Variability of internal wave-driven mixing and stratification in Canadian Arctic shelf and shelf-slope waters. *Journal of Geophysical Research: Oceans*, 123, 9178–9195. <https://doi.org/10.1029/2018JC014342>

Cole, S. T., Toole, J. M., Lele, R., Timmermans, M.-L., Gallaher, S. G., Stanton, T. P., et al. (2017). Ice and ocean velocity in the Arctic marginal ice zone: Ice roughness and momentum transfer. *Elementa: Science of the Anthropocene*, 5, 55. <https://doi.org/10.1525/elementa.241>

D’Asaro, E. A., & Morison, J. H. (1992). Internal waves and mixing in the Arctic Ocean. *Deep-Sea Research Part I Oceanographic Research Papers*, 39(2), S459–S484. [https://doi.org/10.1016/S0198-0149\(06\)80016-6](https://doi.org/10.1016/S0198-0149(06)80016-6)

Dosser, H. V., & Rainville, L. (2016). Dynamics of the changing near-inertial internal wave field in the Arctic Ocean. *Journal of Physical Oceanography*, 46(2), 395–415. <https://doi.org/10.1175/JPO-D-15-0056.1>

Fer, I. (2009). Weak vertical diffusion allows maintenance of cold halocline in the Central Arctic. *Atmospheric and Oceanic Science Letters*, 2(3), 148–152. <https://doi.org/10.1080/16742834.2009.11446789>

Fer, I., Skogseth, R., & Geyer, F. (2010). Internal waves and mixing in the marginal ice zone near the Yermak Plateau. *Journal of Physical Oceanography*, 40(7), 1613–1630. <https://doi.org/10.1175/2010JPO4371.1>

Fine, E. C., Alford, M. H., MacKinnon, J. A., & Mickett, J. B. (2021). Microstructure mixing observations and finescale parameterizations in the Beaufort Sea. *Journal of Physical Oceanography*, 51(1), 19–35. <https://doi.org/10.1175/JPO-D-19-0233.1>

Gregg, M. C. (1989). Scaling turbulent dissipation in the thermocline. *Journal of Geophysical Research*, 94(C7), 9686. <https://doi.org/10.1029/JC094iC07p09686>

Guthrie, J. D., Morison, J. H., & Fer, I. (2013). Revisiting internal waves and mixing in the Arctic Ocean. *Journal of Geophysical Research: Oceans*, 118, 3966–3977. <https://doi.org/10.1002/jgrc.20294>

Ivey, G. N., Winters, K. B., & Koseff, J. R. (2008). Density stratification, turbulence, but how much mixing? *Annual Review of Fluid Mechanics*, 40(1), 169–184. <https://doi.org/10.1146/annurev.fluid.39.050905.110314>

Kawaguchi, Y., Nishino, S., Inoue, J., Maeno, K., Takeda, H., & Oshima, K. (2016). Enhanced diapycnal mixing due to near-inertial internal waves propagating through an anticyclonic eddy in the ice-free Chukchi Plateau. *Journal of Physical Oceanography*, 46(8), 2457–2481. <https://doi.org/10.1175/JPO-D-15-0150.1>

Kowalik, Z., & Proshutinsky, A. Y. (2013). The Arctic Ocean tides. In O. M. Johannessen, R. D. Muench, & J. E. Overland (Eds.), *Geophysical monograph series* (pp. 137–158). Washington, DC: American Geophysical Union. <https://doi.org/10.1029/GM085p0137>

Krishfield, R., Toole, J., Proshutinsky, A., & Timmermans, M.-L. (2008). Automated Ice-Tethered Profilers for seawater observations under pack ice in all seasons. *Journal of Atmospheric and Oceanic Technology*, 25(11), 2091–2105. <https://doi.org/10.1175/2008JTECH0587.1>

Kunze, E. (2017). Internal-wave-driven mixing: Global geography and budgets. *Journal of Physical Oceanography*, 47(6), 1325–1345. <https://doi.org/10.1175/JPO-D-16-0141.1>

Kunze, E., Firing, E., Hummon, J. M., Chereskin, T. K., & Thurnherr, A. M. (2006). Global abyssal mixing inferred from lowered ADCP shear and CTD strain profiles. *Journal of Physical Oceanography*, 36(8), 1553–1576. <https://doi.org/10.1175/JPO2926.1>

Kwok, R. (2018). Arctic sea ice thickness, volume, and multiyear ice coverage: Losses and coupled variability (1958–2018). *Environmental Research Letters*, 13(10), 105005. <https://doi.org/10.1088/1748-9326/aae3ec>

Kwok, R., Spreen, G., & Pang, S. (2013). Arctic sea ice circulation and drift speed: Decadal trends and ocean currents. *Journal of Geophysical Research: Oceans*, 118, 2408–2425. <https://doi.org/10.1002/jgrc.20191>

Lenn, Y. D., Wiles, P. J., Torres-Valdes, S., Abrahamsen, E. P., Rippeth, T. P., Simpson, J. H., et al. (2009). Vertical mixing at intermediate depths in the Arctic boundary current. *Geophysical Research Letters*, 36, L05601. <https://doi.org/10.1029/2008GL036792>

Lincoln, B. J., Rippeth, T. P., Lenn, Y.-D., Timmermans, M. L., Williams, W. J., & Bacon, S. (2016). Wind-driven mixing at intermediate depths in an ice-free Arctic Ocean. *Geophysical Research Letters*, 43, 9749–9756. <https://doi.org/10.1002/2016GL070454>

Martin, T., Tsamados, M., Schroeder, D., & Feltham, D. L. (2016). The impact of variable sea ice roughness on changes in Arctic Ocean surface stress: A model study. *Journal of Geophysical Research: Oceans*, 121, 1931–1952. <https://doi.org/10.1002/2015JC011186>

Martini, K. I., Simmons, H. L., Stoudt, C. A., & Hutchings, J. K. (2014). Near-inertial internal waves and sea ice in the Beaufort Sea. *Journal of Physical Oceanography*, 44(8), 2212–2234. <https://doi.org/10.1175/JPO-D-13-0160.1>

Osborn, T. R. (1980). Estimates of the local rate of vertical diffusion from dissipation measurements. *Journal of Physical Oceanography*, 10(1), 83–89. [https://doi.org/10.1175/1520-0485\(1980\)010<0083:EOTLRO>2.0.CO;2](https://doi.org/10.1175/1520-0485(1980)010<0083:EOTLRO>2.0.CO;2)

Perovich, D. K., & Richter-Menge, J. A. (2009). Loss of sea ice in the Arctic. *Annual Review of Marine Science*, 1(1), 417–441. <https://doi.org/10.1146/annurev.marine.010908.163805>

- Polyakov, I. V., Pnyushkov, A. V., Alkire, M. B., Ashik, I. M., Baumann, T. M., Carmack, E. C., et al. (2017). Greater role for Atlantic inflows on sea-ice loss in the Eurasian Basin of the Arctic Ocean. *Science*, 356(6335), 285–291. <https://doi.org/10.1126/science.aai8204>
- Polyakov, I. V., Rippeth, T. P., Fer, I., Alkire, M. B., Baumann, T. M., Carmack, E. C., et al. (2020). Weakening of cold halocline layer exposes sea ice to oceanic heat in the Eastern Arctic Ocean. *Journal of Climate*, 33(18), 8107–8123. <https://doi.org/10.1175/JCLI-D-19-0976.1>
- Polyakov, I. V., Rippeth, T. P., Fer, I., Baumann, T. M., Carmack, E. C., Ivanov, V. V., et al. (2020). Intensification of near-surface currents and shear in the Eastern Arctic Ocean. *Geophysical Research Letters*, 47, e2020GL089469. <https://doi.org/10.1029/2020GL089469>
- Polzin, K. L., Naveira Garabato, A. C., Huussen, T. N., Sloyan, B. M., & Waterman, S. (2014). Finescale parameterizations of turbulent dissipation. *Journal of Geophysical Research: Oceans*, 119, 1383–1419. <https://doi.org/10.1002/2013JC008979>
- Polzin, K. L., Toole, J. M., & Schmitt, R. W. (1995). Finescale parameterizations of turbulent dissipation. *Journal of Physical Oceanography*, 25, 306–328. [https://doi.org/10.1175/1520-0485\(1995\)025<0306:FPOTD>2.0.CO;2](https://doi.org/10.1175/1520-0485(1995)025<0306:FPOTD>2.0.CO;2)
- Rainville, L., Lee, C., & Woodgate, R. (2011). Impact of wind-driven mixing in the Arctic Ocean. *Oceanography*, 24(3), 136–145. <https://doi.org/10.5670/oceanog.2011.65>
- Rainville, L., & Winsor, P. (2008). Mixing across the Arctic Ocean: Microstructure observations during the Beringia 2005 Expedition. *Geophysical Research Letters*, 35, L08606. <https://doi.org/10.1029/2008GL033532>
- Rainville, L., & Woodgate, R. A. (2009). Observations of internal wave generation in the seasonally ice-free Arctic. *Geophysical Research Letters*, 36, L23604. <https://doi.org/10.1029/2009GL041291>
- Rippeth, T. P., Lincoln, B. J., Lenn, Y.-D., Green, J. A. M., Sundfjord, A., & Bacon, S. (2015). Tide-mediated warming of Arctic halocline by Atlantic heat fluxes over rough topography. *Nature Geoscience*, 8(3), 191–194. <https://doi.org/10.1038/ngeo2350>
- Rudels, B., Anderson, L. G., & Jones, E. P. (1996). Formation and evolution of the surface mixed layer and halocline of the Arctic Ocean. *Journal of Geophysical Research*, 101(C4), 8807–8821. <https://doi.org/10.1029/96JC00143>
- Shibley, N. C., Timmermans, M.-L., Carpenter, J. R., & Toole, J. M. (2017). Spatial variability of the Arctic Ocean's double-diffusive staircase. *Journal of Geophysical Research: Oceans*, 122, 980–994. <https://doi.org/10.1002/2016JC012419>
- Sirevaag, A., & Fer, I. (2012). Vertical heat transfer in the Arctic Ocean: The role of double-diffusive mixing. *Journal of Geophysical Research*, 117, C07010. <https://doi.org/10.1029/2012JC007910>
- Stroeve, J. C., Kattsov, V., Barrett, A., Serreze, M., Pavlova, T., Holland, M., & Meier, W. N. (2012). Trends in Arctic sea ice extent from CMIP5, CMIP3 and observations. *Geophysical Research Letters*, 39, L16502. <https://doi.org/10.1029/2012GL052676>
- Timmermans, M.-L. (2015). The impact of stored solar heat on Arctic sea ice growth. *Geophysical Research Letters*, 42, 6399–6406. <https://doi.org/10.1002/2015GL064541>
- Timmermans, M.-L., Proshutinsky, A., Krishfield, R. A., Perovich, D. K., Richter-Menge, J. A., Stanton, T. P., & Toole, J. M. (2011). Surface freshening in the Arctic Ocean's Eurasian Basin: An apparent consequence of recent change in the wind-driven circulation. *Journal of Geophysical Research*, 116, C00D03. <https://doi.org/10.1029/2011JC006975>
- Timmermans, M.-L., Toole, J., & Krishfield, R. (2018). Warming of the interior Arctic Ocean linked to sea ice losses at the basin margins. *Science Advances*, 4(8), eaat6773. <https://doi.org/10.1126/sciadv.aat6773>
- Timmermans, M.-L., Toole, J., Krishfield, R., & Winsor, P. (2008). Ice-Tethered Profiler observations of the double-diffusive staircase in the Canada Basin thermocline. *Journal of Geophysical Research*, 113, C00A02. <https://doi.org/10.1029/2008JC004829>
- Toole, J., Krishfield, R., Timmermans, M.-L., & Proshutinsky, A. (2011). The Ice-Tethered Profiler: Argo of the Arctic. *Oceanography*, 24(3), 126–135. <https://doi.org/10.5670/oceanog.2011.64>
- Toole, J. M., Timmermans, M.-L., Perovich, D. K., Krishfield, R. A., Proshutinsky, A., & Richter-Menge, J. A. (2010). Influences of the ocean surface mixed layer and thermohaline stratification on Arctic sea ice in the central Canada Basin. *Journal of Geophysical Research*, 115, C10018. <https://doi.org/10.1029/2009JC005660>
- Waterhouse, A. F., MacKinnon, J. A., Nash, J. D., Alford, M. H., Kunze, E., Simmons, H. L., et al. (2014). Global patterns of diapycnal mixing from measurements of the turbulent dissipation rate. *Journal of Physical Oceanography*, 44(7), 1854–1872. <https://doi.org/10.1175/JPO-D-13-0104.1>
- Whalen, C. B., de Lavergne, C., Naveira Garabato, A. C., Klymak, J. M., MacKinnon, J. A., & Sheen, K. L. (2020). Internal wave-driven mixing: Governing processes and consequences for climate. *Nature Reviews Earth and Environment*, 1, 606. <https://doi.org/10.1038/s43017-020-0097-z>
- Whalen, C. B., MacKinnon, J. A., & Talley, L. D. (2018). Large-scale impacts of the mesoscale environment on mixing from wind-driven internal waves. *Nature Geoscience*, 11(11), 842–847. <https://doi.org/10.1038/s41561-018-0213-6>
- Whalen, C. B., MacKinnon, J. A., Talley, L. D., & Waterhouse, A. F. (2015). Estimating the mean diapycnal mixing using a finescale strain parameterization. *Journal of Physical Oceanography*, 45(4), 1174–1188. <https://doi.org/10.1175/JPO-D-14-0167.1>
- Whalen, C. B., Talley, L. D., & MacKinnon, J. A. (2012). Spatial and temporal variability of global ocean mixing inferred from Argo profiles. *Geophysical Research Letters*, 39, L18612. <https://doi.org/10.1029/2012GL053196>